

# Extending EDRS to Laser Communication from Space to Ground

Zoran Sodnik and Marc Sans

European Space Agency (ESA)  
European Space Technology and Research Centre (ESTEC)  
2200AG Noordwijk, The Netherlands  
zoran.sodnik@esa.int

**Abstract**— The European Data Relay Satellite (EDRS) system will utilize laser communications for inter-satellite links in space and radio frequency communications from space to ground. In order to extend the coherent laser links from space to ground atmospheric distortions need to be compensated. This paper discusses alternative ways of atmospheric turbulence mitigation and focuses on the Multimode Differential Phase-Shift Encoding (M-DPSE) technique that will be tested in ESA's Optical Ground Station (OGS).

**Keywords**— M-DPSE; Alphasat; EDRS; laser communication terminals; free-space optical communications; space to ground communications

## I. INTRODUCTION

The European Data Relay Satellite (EDRS) system, which will be deployed starting from 2015, will initially consist of two spacecraft in Geostationary Earth Orbit (GEO). The orbital locations of EDRS-A and EDRS-C will be 9 degrees East and 31 degrees East respectively. EDRS will be the first operational data-relay system utilizing inter-satellite laser communications technology and it will service the Sentinel 1a and 2a Earth observation spacecraft in Low Earth Orbit (LEO) as well as its successors (Sentinel 1b and 2b), see Figure 1.



Fig. 1. Artist's impression of EDRS data relay services.

A precursor data-relay Technology Demonstration Package (TDP#1) will be launched in the first half of 2013 on the Alphasat satellite in GEO (25 degrees East).

The Laser Communication Terminals (LCT) used on Alphasat and EDRS are developed by Tesat Spacecom under contract from the German Space Agency (DLR). They utilize Binary Phase Shift Keying (BPSK) modulation and coherent homodyne detection scheme, one of the most sensitive modulation formats (in terms of photons per bit required).

Two precursor LCTs are flying since 2007 onboard the LEO satellites TerraSAR-X and NFIRE and are demonstrating inter-satellite communications at data rates of 5.625 Gbps (up to 6000 km distance) [1], [2], [3].

While very well suited for high data-rate inter-satellite communication links, BPSK is not ideal when it comes to space to ground link applications, because the phase integrity (wave-front) of a beam is compromised when passing atmospheric turbulence. Phase integrity is vital for BPSK demodulation; otherwise the interference contrast in the receiver (when mixing with a local oscillator laser) is deteriorated and data can only be decoded reliably in case of very good seeing conditions.

## II. ATMOSPHERIC TURBULENCE MITIGATION

The necessity to mitigate atmospheric turbulence applies to all laser modulation formats if high data-rates (in the gigabits per second range) are transmitted, because then receivers either need a coherent detection scheme or have to use single-mode fiber-coupled pre-amplifiers to reach the signal to noise levels required. It can easily be shown that loss of interference contrast and loss of single-mode fiber-coupling efficiency are identical phenomena when wave-fronts are distorted.

The following possibilities exist to mitigate that problem.

### A. Small Receive Aperture

The most simple solution is to reduce the diameter of the receive aperture on ground below the size of the Fried parameter (a measure of atmospheric turbulence strength which defines – in terms of resolution – the useful diameter of a telescope). In that case wave-front deformations caused by atmospheric turbulence only create angle-of-arrival fluctuations that can be corrected by tip/tilt control. The



communications by NASA for its Laser Communication Relay Demonstration (LCRD). It is based on interference of successive data bits in an unequal arm-length interferometer, where the optical path difference (OPD) in the interferometer corresponds to the duration of one bit. The coherence length of the laser light needs to be much longer than the OPD, which needs to be stabilized in the interferometer to a fraction of the wavelength. The relative phases of two successive data bits are converted into intensity by interference. If the phases of two successive bits are identical the result is constructive interference, while if two successive bits are different the output will be destructive interference. However, as the encoding of the data is Binary Phase Shift Keying (BPSK) and not DPSK, the received bit sequence becomes the derivative of the bit sequence sent.

While DPSK is used in single mode operation only M-DPSE operates equally well in multi-mode conditions if the two interfering bits experience identical wave-front distortions. One way to achieve that is pupil imaging [7].

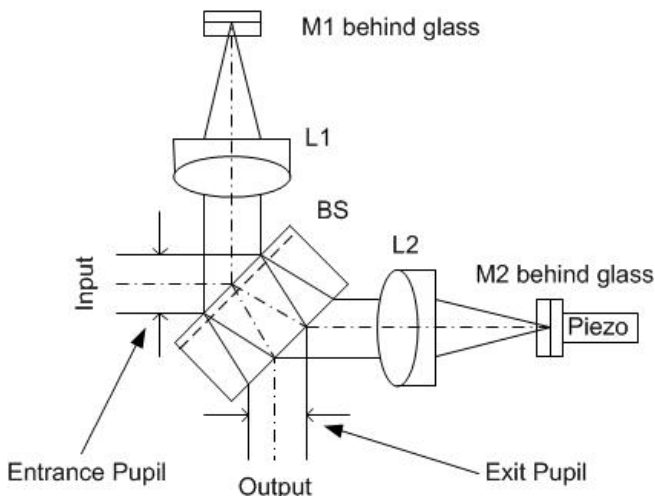


Fig. 3. Schematic drawing of the M-DPSE system based on a Michelson interferometer.

A schematic drawing of a multi-mode Michelson type interferometer with unequal arm-length is shown in Figure 3. Each interferometer arm uses a single achromatic lens to re-image the pupil. The focal lengths of the lenses together with the thickness of the beam-splitter plate are selected to achieve the required OPD and to maintain identical location of the output pupil. In principle the location of input pupil and output pupil can be placed anywhere, as long as they are identical in position and size for both interferometer arms. Mirror M2 is controlled by a Piezo-crystal to maintain the operational bias point in the interferometer to a fraction of the wavelength despite Doppler shift of the light received [8]. Both mirrors are covered by a thin glass plate in order to prevent dust particles from disabling the interferometer (at the beam focus).

The modulation contrast in an interferometer depends on interference of identical wave-fronts, not on the quality of the wave-front itself. To maintain identical wave-fronts, the

entrance pupil is imaged in both arms onto the same exit pupil. This ensures that the interferometer superimposes identical wave-fronts (within the bit duration the wave-front cannot change because atmospheric turbulence effects are much slower) and optimum modulation contrast is obtained despite a distorted input wave-front.

While the M-DPSE solves the interference contrast problem, it does not remove atmospheric wave-front distortions and focusing into the tiny mode field area of a single-mode fiber is still not possible. However, the sensitive area of high speed ( $\leq 10$  Gbps) photo-detectors is much larger and the net gain of the M-DPSE technique is therefore given by the area ratio between photo-detector and diffraction limited point spread (Airy-) function. While the diameter of the photo-detector (onto which the light from the interferometer is focused) is  $60 \mu\text{m}$ , the mode field diameter of a single mode fiber (NA=0.15) at that 1064 nm wavelength would be around  $10 \mu\text{m}$ .

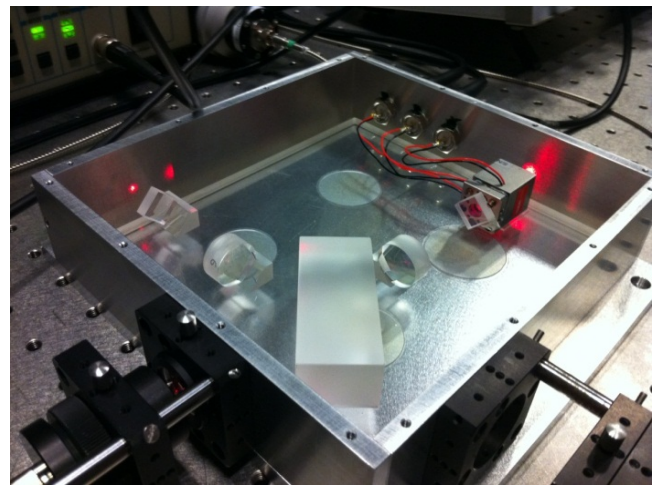


Fig. 4. Michelson interferometer with pupil-imaging lenses in both arms. The entrance aperture is in the lower left and the exit aperture is in the lower right. The beam splitting plate, the pupil imaging lenses and the end mirrors (one with piezo-control) are visible.

Figure 4 shows a M-DPSE Michelson-type interferometer developed for the reception of Binary Phase Shift Keying (BPSK) modulated data from laser communication terminals on-board the TerraSAR-X and NFIRE satellites. The wavelength used is 1064 nm and the data rate is 5.625 Gbps.

This system has been successfully tested with turbulence generators to verify the M-DPSE principle.

### III. IMPLEMENTATION OF M-DPSE IN ESA'S OGS

The M-DPSE interferometer which will be installed at ESA's Optical Ground Station will provide the ERDS project with a relatively simple commissioning and testing facility for their laser communication terminals on-board the Alphasat, ERDS-A and EDRS-C satellites. The OGS has already performed similar tasks with LCTs on-board the ARTEMIS, OICETS, TerraSAR-X and NFIRE satellites [9], [10], [11]. Being a ground based facility, the OGS can also measure

received beam parameters, such as central wavelength, wavelength stability and polarization as well as the acquisition and communication timing [12]. The 1 meter Zeiss telescope of the OGS is shown in Figure 5.



Fig. 5. 1 meter Zeiss telescope of the OGS

The physical location and the communication parameters of the OGS are summarized in Table 1.

TABLE I. OPTICAL GROUND STATION SPECIFICATIONS

Parameter	Value	Unit
Geographic longitude	16° 30' 36.36"	West
Geographic latitude	28° 17' 58.29"	North
Altitude above sea level	2393	m
Receiver telescope diameter	1016	mm
Receiver focal length	39000	mm
Transmitter diameter	39	mm
Transmitter laser power	50	W
Communication wavelength	1064	nm
Communication data rate	2.8125	Gbps

#### A. Further M-DPSK Simplification

The Michelson type M-DPSK interferometer presented in Figures 3 and 4 can be further simplified because pupil imaging is actually not required. This was proposed by Kyliä, the French company that built the M-DPSK interferometer under ESA contract.

Refractive properties of a glass substrate in one arm of the interferometer can be utilized to perform two functions, namely:

- to provide the required OPD between interferometer arms;
- to maintaining identical etendue in both interferometer arms;

The M-DPSK interferometer, which will be built for decoding laser communication data from Alphasat and EDRS, is shown in Figure 6. It utilizes a beam-splitter cube (BSC), a glass block mirror (GBM) in one arm and a piezo-crystal controlled standard mirror (M1) in the other.

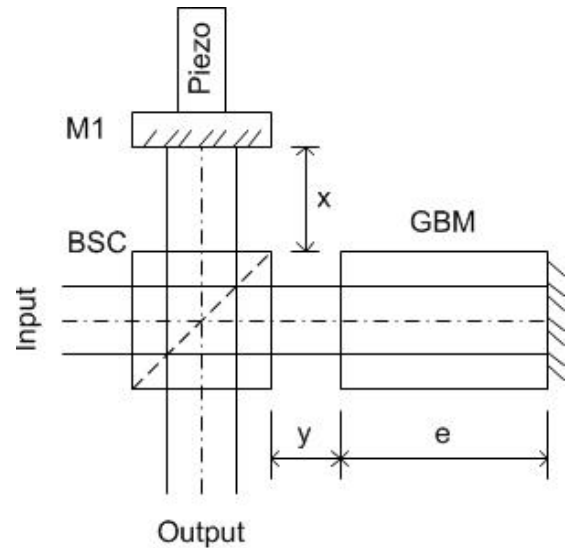


Fig. 6. M-DPSK interferometer design.

To satisfy the OPD as well as the etendue requirements, the following interferometer component dimensions have to be fulfilled:

$$2y + 2n \cdot e - 2x = OPD \quad (1)$$

$$2y + \frac{2e}{n} - 2x = 0 \quad (2)$$

With (y) the distance between the beam splitter cube and the glass block mirror, (e) the length of the glass block mirror of refractive index (n) and (x) the distance between the beam splitter cube and mirror M1. Combining equations 1 and 2 one gets the following interferometer dimensions:

$$x - y = \frac{OPD}{2(n^2 - 1)} \quad (3)$$

$$e = n \cdot (x - y) \quad (4)$$

For N-BK7 (with an index of refraction of  $n = 1.5067$  at 1064 nm) the differential component separation in the interferometer arms becomes  $x - y = 41.962$  mm and the thickness of the glass block mirror  $e = 63.224$  mm. For ultimate compactness the y dimension can be reduced to zero making one interferometer arm monolithic.

It can easily be shown that dimensional requirements are both violated with the cosine of the field angle where the error becomes 1% at a field angle of 8 degrees. Assuming a 1 meter aperture, as shown in Figure 5, and a telescope magnification

of 100, a 1% error is reached when the external telescope field angle becomes  $\pm 4.8$  arcmin. However this only applies to higher order wave-front errors as tip/tilt is removed via a control loop.

In simple terms the “lens-less” M-DPSK interferometer design maintains identical beam properties (etendue) at the interferometer output despite the optical path difference (OPD) of the interferometer arms. The lack of pupil imaging requires a somewhat larger aperture lens system that focuses the light onto a detector caused by higher order wave-front distortions that are not compensated by tip/tilt.

**B. Receiver design**

Figure 7 shows the focal plane instrumentation with M-DPSE interferometer that will be installed in the Coudé beam path of ESA’s Optical Ground Station (OGS) telescope.

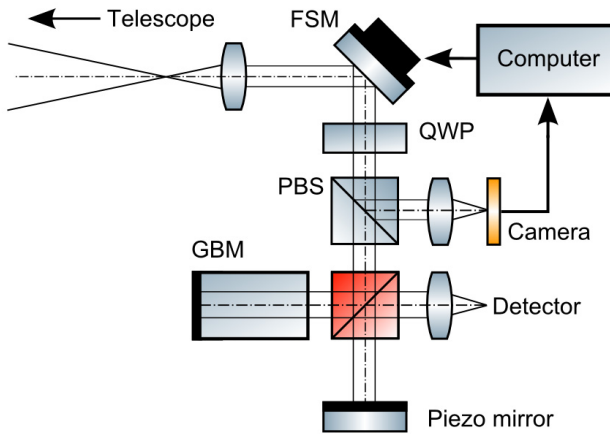


Fig. 7. Focal plane instrumentation with M-DPSE.

The light from the telescope’s primary focus is collimated and tip/tilt correction is performed at the internal pupil using a fine steering mirror (FSM). After reflection by the FSM, the circularly polarized beam passes a quarter wave plate (QWP) which converts it into linearly polarized light.

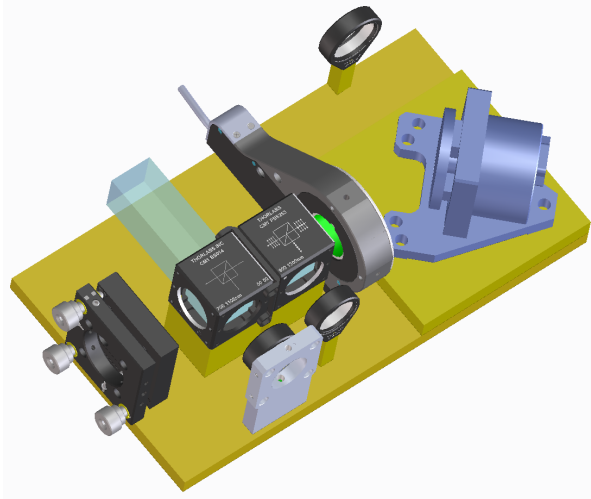


Fig. 8. Mechanical design of the focal plane instrumentation

By motorized rotation of the QWP the splitting ratio of a polarizing beam splitter (PBS) is adjusted for optimum power distribution between Camera and M-DPSE interferometer. The focal plane instrumentation is shown in Figure 8.

The interferometer output is focused onto an (10 Gbps) avalanche photo-Detector (Discovery Semiconductors), where the derivative of the originally transmitted BPSK bit sequence is recorded. The bit sequence derivative is caused by the differential detection principle of the M-DPSE interferometer, if BPSK modulation is applied as input. The signal is amplified and passes data and clock recovery electronics before bitwise integration is performed to retrieve the original bit sequence.

Figure 9 shows a principle sketch of the electronics circuit design for bit sequence integration. It has been developed using evaluation boards of high frequency dual D-type flip/flop and an XOR gates (Hittite Corp.).

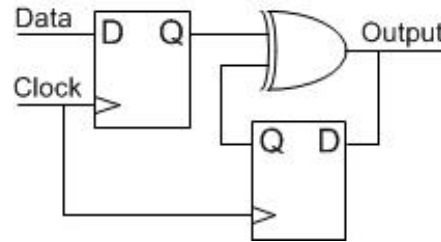


Fig. 9. Synchronous high speed bit integration circuit

**C. Transmitter design**

The transmitter is completely separated from the receiver in order to minimize stray-light from the fiber amplifier (50 Watts) to enter the receive telescope. A 1064 nm seed laser, based on a Nd:YAG non-planar ring oscillator (Mephisto) is fiber coupled to a phase modulator (Northrop Grumman Corp.). The phase modulator output is routed via a long polarization maintaining single-mode fiber to the side of the telescope tube, where the fiber amplifier (Nufem) and the laser transmitter system are also attached, as shown in Figure 10.

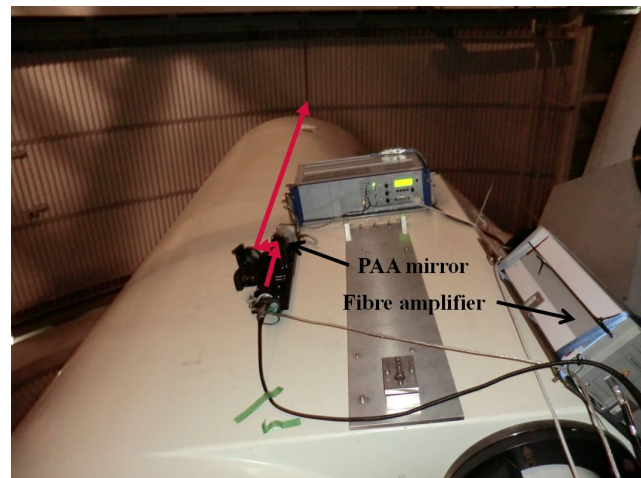


Fig. 10. Transmitter system as installed at the OGS telescope for TerraSAR-X and NFIRE satellite communication experiments

#### D. Transmitter/receiver alignment

In order to align the optical axes of transmitter and receiver a high precision ( $<1$  arcsecond) corner-cube retro-reflector (CCRR) bar as shown in Figure 11 will be placed in front of the 39 mm diameter transmit beam such that the retro-reflected beam is laterally shifted and enters the telescope aperture. A retro-reflector bar can be seen as a cut-out of a large CCRR. It is used for lateral displacement of the retro-reflected beam, while maintaining perfect parallelism. Diffraction will enlarge the point spread function (PSF) on the camera from each transmit beam by a factor of 30 beyond the PSF diameter from a satellite, which needs to be taken into account during alignment. However, the diameter represents the true far field divergence of the transmit beam.

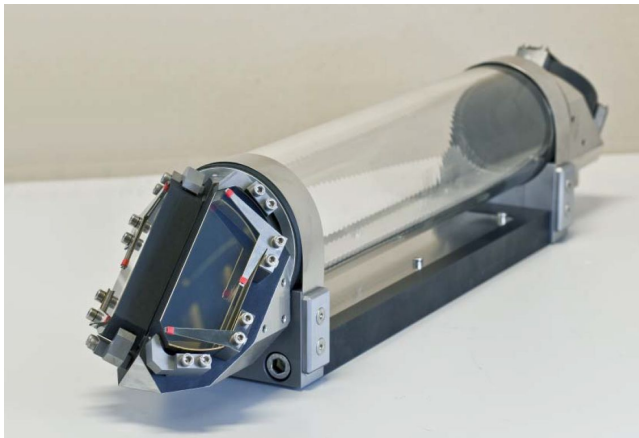


Fig. 11. Corner-cube retro-reflector bar made from Zerodur for thermal and mechanical stability with 50 cm length and 50 mm aperture.

#### IV. CONCLUSIONS

This novel detection concept may well become the enabling technology for using coherent modulation techniques through atmospheric turbulence. It may pave the way for the implementation of inexpensive ground-based optical telescope receivers for cloud coverage mitigation by meteorological space diversity. The detection principle can also be used with non-diffraction limited telescopes and large apertures.

#### ACKNOWLEDGMENT

The authors would like to thank the company Kyliia (Paris) for the development of the first prototype of the M-DPSE interferometer and acknowledge the most valuable contributions from Aurélien Boutin. We would also like to thank Jyri Kuusela and David Abreu from Ataman Science for the development and testing of a Novel Optical Receiver Assembly (NORA) based upon the M-DPSK interferometer and Bernhard Wandernoth from Synopta for his consultancy in high-speed detection technology.

#### REFERENCES

- [1] R. Lange, B. Smutny, "Homodyne BPSK-based optical inter-satellite communication links", Proc. SPIE 6457, (2007).
- [2] B. Smutny et al, "In-orbit verification of optical inter-satellite communication links based on homodyne BPSK", Proc. SPIE vol. 6877, (2008).
- [3] B. Smutny et al, "5.6 Gbps optical inter-satellite communication link", Proc. SPIE vol. 7199, (2009).
- [4] R. Fields, D. Kozlowski, H. Yura, R. Wong, J. Wicker, C. Lunde et al., "5.625 Gbps Bidirectional Laser Communications Measurements Between the NFIRE Satellite and an Optical Ground Station" IEEE Proc. pp. 44–53, (2011).
- [5] N. Devaney et al., "Correction of ocular and atmospheric wavefronts: a comparison of the performance of various deformable mirrors", Appl. Opt. 47, 6550-6562 (2008).
- [6] Th. Berkefeld, D. Soltau, R. Czichy, E. Fischer, B. Wandernoth and Z. Sodnik, "Adaptive optics for satellite-to-ground laser communication at the 1m Telescope of the ESA Optical Ground Station, Tenerife, Spain", Proc. SPIE vol. 7736, (2010).
- [7] Z. Sodnik, J. Perdigues, R. Czichy, and R. Meyer, "Adaptive Optics and ESA's Optical Ground Station", Proc. SPIE vol. 7464, (2009).
- [8] T. Rose, C. Klimcak, D. Kozlowski, G. Seffler, H. Yura, A. Walston, N. Werner and C. Mueller, "Wavelength Tracking Interferometer for DPSK" IEEE Proc. pp. 308–313, (2011).
- [9] J. Romba, Z. Sodnik, M. Reyes, A. Alonso and A. Bird, "ESA's Bidirectional Space-to-Ground Laser Communication Experiments", Proc. SPIE vol. 5550, (2004).
- [10] A. Alonso, M. Reyes and Z. Sodnik, "Performance of satellite-to-ground communications link between ARTEMIS and the Optical Ground Station", Proc. SPIE vol. 5572, (2004).
- [11] Z. Sodnik, H. Lutz, B. Furch and R. Meyer, "Optical Satellite Communications in Europe", Proc. SPIE vol. 7587, (2010).
- [12] R. Czichy, Z. Sodnik and B. Furch, "Design of an Optical Ground Station for In-Orbit Check-Out of Free Space Laser Communication Payloads", Proc. SPIE vol. 2181, (1995).